A closer comparison of early and late winter atmospheric trends in the Northern-Hemisphere

Yongyun Hu

NASA Goddard Institute for Space Studies

and Center for Climate Systems Research

Columbia University

2880 Broadway, 112th Street

New York, NY 10025

Ka Kit Tung

Department of Applied Mathematics

University of Washington

P.O. Box 352420

Seattle, WA 98195-2420

Jiping Liu

School of Earth & Atmospheric Sciences

Georgia Institute of Technology

311 Ferst Drive

Atlanta, GA 30332-0340

Short title: CLIMATE, TRENDS, WAVES, CIRCULATIONS

Abstract. We compare decadal trends in various fields between Northern-Hemisphere early winter (November-December, ND) and late winter(February-March, FM)months using observational reanalysis data. It is found that in the extratropics and polar region the decadal trends display nearly opposite tendencies between ND and FM. Trends in FM are associated a colder and stronger polar vortex and weaker wave fluxes from the troposphere to the stratosphere, consistent with a positive trend of the Arctic Oscillation (AO), as found in earlier studies, while trends in ND appear to resemble a trend toward the low-index polarity of the AO. In the tropics, the Hadley circulation shows significant intensification in both ND and FM, with stronger intensification in FM. Unlike the Hadley cell, the Ferrel cell shows opposite trends between ND and FM, with weakening in ND and strengthening in FM. Comparison of the observational results with general circulation model simulations are also discussed.

1. Introduction

Recent studies showed noticeable trends in Northern-Hemisphere (NH) winter and springtime (e.g., January-February-March (JFM)) during the past few dacades. At the surface, air temperatures warmed over the NH high-latitude continents (Hurrel, 1995, Jones *et al.*, 1999, Thompson, *et al.*, 2000). The stratospheric Arctic experienced strong cooling in late winter and springtime, associated with Arctic ozone depletion (Pawson and Naujokat, 1999, Randel and Wu, 1999, Labitzke and Naujokat, 2000). The stratospheric polar night jet strengthened (Waugh *et al.*, 1999), corresponding to decreased wave activity in the extratropics in both the troposphere and the stratosphere (Zhou *et al.*, 2001, Randel *et al.*, 2002, Hu and Tung, 2003). It was suggested that these trends from the surface to the stratosphere are dynamically linked through troposphere-stratosphere interaction, and that they are associated with the Arctic oscillation (AO) (Thompson, *et al.*, 2000, Hartmann *et al.*, 2000, Wallace and Thompson, 2002). These studies, together with others (Baldwin and Dunkerton,2001, Kodera and Kuroda, 2000, Hu and Tung, 2003, Coughlin and Tung, 2004), have emphasized the possible dynamical influence of the stratosphere on the troposphere.

Since the trends in JFM have high statistical significance, Hartmann *et al.* (2000) suggested that these trends likely exceed their natural variability and thus might be caused by external forcing. The question of what could be the external forcing responsible for these observed trends has motivated various general circulation model (GCM) simulation studies. These studies have mainly focused on testing three possible major forcings: increasing greenhouse gases (Shindell *et al.*, 1999, Gillett *et al.*, 2002, Butchart, 2000), stratospheric ozone depletion (Graf *et al.*, 1998, Volodin and Galin, 1999), and tropical sea surface temperature (SST) warming (Fyfe *et al.*, 1999, Horeling *et al.*, 2001, Schneider, 2003). Briefly, these simulation studies are primarily interested in the radiative effects from changes in atmospheric trace gases or from changes in tropical sea-surface temperatures on atmospheric circulations and regional climate, and are concerned with the impact of the tropics on the extratropics and the influence of the stratosphere on the troposphere.

Decadal trends are also found in early-winter months (November-December, ND). Although mainly focusing on the decadal trends in JFM, Zhou *et al.* (2001), Randel *et*

al. (2002), and Hu and Tung (2002), also commented on the trends in ND. Zhou *et al.* (2001) showed that wave activity in ND have trends opposite to that in JFM. Randel *et al.* (2002) and Hu and Tung (2002, 2003) found that planetary wave activity at high latitudes exhibited positive trends in ND, while showing negative trends in JFM. In contrast to intensive studies on the trends in JFM, trends in early winter have received little attention. Our main goal in this study is to make a closer comparison of decadal trends in various fields and demonstrate their striking contrast between early-winter and late-winter months. In particular, we broaden the analysis of decadal trends in our previous studies (Hu and Tung, 2002, 2003), in which our interests were in the relationship between wave activity in the high-latitude stratosphere and polar temperatures. In the present study, our trend analysis extends to the tropospheric tropics and the midlatitudes. One of our interests is to demonstrate the connection of trends in both meridional and vertical directions by studying spatial structures of trends in the meridional-vertical plane. To sharpen the contrast of trends between early and late winter, we choose ND and FM to represent early and late winter, respectively. As we will show, January appears to be a transitional period.

The surface air temperature (SAT) data used in this study is from the analysis at Goddard Institute for Space Studies. The others are reanalyses from the National Center for Environmental Prediction/National Center for Atmospheric Research (NCEP/NCAR). Our linear-trend calculations in the present study are 25 years from the 1978-1979 winter to the 2002-2003 winter. Thus, trends for ND and FM are calculated over 1978-2002 and 1979-2003, respectively.

2. Results

2.1. Trends in zonal-mean temperatures

Figure 1 shows the 25-year trend in zonal-mean temperatures at 50 mb (about 21 km high) as a function of latitudes and months. The trends exhibit cooling over most of the globe, with particularly strong cooling trends in both polar regions in the late winter and springtime, i.e., FM for the Arctic and October-November for the Antarctic. Warming trends, however, are found in both polar regions during early-winter months, i.e., ND for

the Arctic and July-August-September for the Antarctic. For the Arctic, it appears that January is an intermediate period transitioning from the early-winter warming to late-winter cooling, with warming during the first half of the month and cooling in the second half. This is partly the reason why January is not included for our current trend analysis. The seasonal-spatial pattern in Figure 1 is similar to the results by Rammaswamy *et al.* (1996) and Randel and Wu (1999) over shorter periods. The similarity of the seasonal-spatial patterns of temperature trends in the Arctic and Antarctic leads to the suggestion that the Arctic cooling may be primarily caused by Arctic ozone depletion (Ramaswamy *et al.*, 1996, Randel and Wu, 1999), though changes in wave-driven dynamical heating may also be an important factor.

Figure 2 a and b show the meridional-vertical plots of the 25-year trends in zonal-mean temperatures in ND and FM, respectively. At stratospheric levels, the tropics and midlatitudes are dominated by statistically significant cooling trends in both ND and FM. Trends in the polar region show opposite tendencies, with warming in ND and strong cooling in FM. In the troposphere, the spatial distributions of temperature trends are nearly opposite between ND and FM. In ND, warming trends are found in the tropics, subtropics, and polar region, with mild cooling trends in midlatitudes. In contrast, in FM the tropical upper troposphere and the polar region show cooling trends, with warming trends in midlatitudes. While the bulk vertical structure of temperature trends in the tropics and midlatitudes, with warming in the troposphere and cooling in the stratosphere, is broadly consistent with what can be expected from the result of greenhouse warming and stratospheric ozone depletion in both ND and FM, trends in the polar region are complicated. The observed polar trends probably cannot be explained by radiative effects alone, because they are also affected by wave fluxes. We will discuss these more later.

The non-uniform spatial pattern of temperature trends leads to changes in meridional temperature gradients. In the stratosphere, the contrast between polar warming and midlatitude cooling in ND indicates weakened temperature gradient at subpolar latitudes, while in FM the contrast of strong Arctic cooling and relatively weak midlatitude cooling suggests enhanced temperature gradients. From Figure 2b, one can find that the temperature contrast crossing subpolar latitudes increased by about 3 or 4 K in the past

25 years in FM. In the troposphere, the contrast between warming trends in the tropics and polar region and cooling trends at midlatitudes in ND mean enhanced temperature gradients in the subtropics and weakened temperature gradients at about 60°N. In FM, the meridional structures of temperature trends indicate weakened temperature gradients in the subtropics and enhanced temperature gradients at about 60°N, opposite to that in ND. It is anticipated that the changes in meridional temperature gradients are accompanied by changes in mean zonal winds.

2.2. Trends in mean zonal winds

Figure 3a and b show the 25-year trends in zonal-mean zonal winds for ND and FM, respectively. For ND, negative trends are found in the mid- and high-latitude stratosphere and subpolar troposphere, with maximum of about -7 ms^{-1} for the 25 years and statistical significance above the 95% confidence level, indicating a largely *decelerated* subpolar jet. The deceleration of subpolar zonal winds is consistent with the weakening of subpolar meridional temperature gradients in Figure 2a, according to the thermal wind relation. Zonal winds show weak positive trends in the subtropical troposphere (between about 30°N and 45°N) and the polar regions. Similarly, the acceleration of zonal winds in the subtropical troposphere is consistent with the enhancement of temperature gradients in the subtropics in Figure 2a.

For FM, mean zonal winds show positive trends in the subpolar stratosphere, with maximum of about 6 ms^{-1} in the subpolar stratosphere. This indicates an *accelerated* polar night jet. The zonal-wind acceleration is well consistent with enhanced temperature gradients near subpolar latitudes shown in Figure 2b. The changes of the stratospheric polar night jet are also reflected in its longer persistence in springtime in recent years. Waugh *et al.* (1999) found that the Arctic vortex breakup is delayed about 15 days over the 1990s. From Figure 3b, one can find that the acceleration of zonal winds extends from the subpolar stratosphere into the extratropical troposphere, tilting poleward with height. The tilting appears to be more pronounced than that of the AO (see Thompson *et al.*, 2000). The simulation work by Kushner and Polvani (2003) suggests that the acceleration of extratropical tropospheric zonal winds involves a feedback between zonal winds and

waves. Mean zonal winds show negative trends in the subtropics and the polar region. The deceleration of subtropical zonal winds corresponds to the weakening of temperature gradients in the subtropics. The trends in mean zonal winds show clear opposite spatial patterns between ND and FM.

2.3. Trends in wave propagation and fluxes

In Hu and Tung (2002, 2003), we focused on time-series analyses of wave activity at high latitudes, i.e., north of 50°N. Here, we are more interested in the spatial pattern of wave flux trends in both vertical and meridional directions. We first study the changes in wave propagation. Changes in wave propagation can be anticipated from the trends in the squared indices of refraction, although it is difficult to infer which is the cause and which is the effect. Regions with positive trends in the indices of refraction tend to be more favorable for wave propagation, while the regions with negative trends tend to refract waves away. Figure 4a shows the trends in wavenumber-1 refractive indices for ND. Positive trends are in the subpolar troposphere and most parts of the stratosphere, with a maximum near the subpolar tropopause. Relatively weak negative trends are in the lower latitudes. Such a spatial distribution of the refractive index trends suggests that the high-latitude extratropics have become more favorable for wave propagation compared to lower latitudes. Thus, planetary waves tend to propagate upward along the subpolar waveguide in ND.

Figure 4b shows the trends in refractive indices for FM. The stratosphere is dominated by negative trends, indicating that in FM the stratosphere has become less favorable for planetary wave propagation in the 25 years. A band of negative trends between 45°N and 65°N extends from the stratosphere into the troposphere. Since this region is the primary channel for upward planetary wave propagation, the negative trends suggest suppressed wave propagation from the troposphere into the stratosphere. While the refractive indices exhibit negative trends in high latitudes, they show weak positive trends in lower latitudes. Such a spatial pattern, opposite to that in ND, indicates that in FM waves tend to propagate more equatorward.

Changes in wave propagation can be more explicitly demonstrated with the trends in Eliassen-Palm (EP) flux vectors, since EP flux vectors approximately point toward the local

directions of wave propagation. The white arrows in Figure 5a and b denote the changes in EP flux vectors over the 25 years. Since the climatological direction of wave propagation in the extratropical troposphere is upward and equatorward, in Figure 5a the poleward arrows in the middle and upper troposphere in the extratropics indicate reduced equatorward wave propagation in ND. The upward arrows in the mid- and high-latitude stratosphere mean enhanced upward wave propagation from the troposphere to the stratosphere. In Figure 5b for FM, the downward arrows in the polar region indicate suppressed upward wave propagation at high latitudes, and the equatorward and upward arrows in the midlatitude upper troposphere indicate enhanced wave propagation toward the subtropical upper troposphere. Indeed, the trends in EP flux vectors are consistent with the trends in the refractive indices. The opposite tendencies in wave propagation were also reported by Zhou *et al.* (2001).

As wave propagation is altered, EP flux divergence, which characterizes the interaction between waves and the zonal-mean flow, may also be changed. The trends in EP flux divergence in ND and FM are shown in Figure 5a and b (background color shading), respectively. In ND, the stratosphere between 45°N and 90°N is dominated by the negative trends, indicating increased EP flux convergence in the mid- and high-latitude stratosphere and corresponding to the deceleration of the polar night jet. As discussed in Hu and Tung (2002), the increasing of EP flux convergence leads to enhanced meridional residual circulation and thus stronger adiabatic heating in the polar region, which causes the polar warming shown in Figure 2a. Positive trends are located in the lower latitudes stratosphere. In the troposphere, the situation is complicated. Nevertheless, one can find negative trends in the upper troposphere between 50°N and 70°N and positive trends in the middle troposphere between 30°N and 50°N. These roughly correspond to the zonal-wind changes in the troposphere shown in Figure 3a.

For FM, positive trends in EP flux divergence (less convergence) are in the high-latitude stratosphere, with negative trends (more convergence) in lower latitudes. This is opposite to that in ND. In the troposphere, positive trends are located in the extratropical troposphere. Large negative trends are in the subtropical upper troposphere between 25°N and 45°N, indicating largely enhanced EP flux convergence in the subtropics. These positive and

negative trends correspond to the zonal-wind acceleration at subpolar latitudes and deceleration in the subtropics, respectively, as shown in Figure 3b. Moreover, the decrease in EP flux convergence in the high-latitude stratosphere indicates a weaker residual circulation and less wave-driven dynamical heating in the stratospheric Arctic. Thus, the strong Arctic cooling shown in Figure 2b can be partly attributed to the decreasing of EP flux convergence in the high-latitude stratosphere.

Since the vertical component of EP fluxes is equivalent to eddy-heat fluxes, in Figure 5a the upward and poleward arrows in the upper troposphere between about 40°N and 50°N indicate enhanced eddy-heat transport from midlatitudes to the polar region, consistent with the midlatitude cooling in the upper troposphere and warming in the polar region, as shown in Figure 2a. In Figure 5b, the upward arrows in the midlatitude upper troposphere mean enhanced poleward eddy-heat fluxes from the subtropics to midlatitudes. Meanwhile, the downward arrows in the polar region mean reduced eddy-heat transport from midlatitudes to the polar region. The two lead to convergence of eddy-heat fluxes at midlatitudes and causes warming in midlatitudes and cooling in the polar region (between about 55°N and 80°N). Thus, the trends in zonal-mean temperatures are consistent with the changes in eddy-heat fluxes.

2.4. Trends in mean meridional circulations

Most of earlier studies on winter-time climate trends in the Northern Hemisphere focused on circulation changes in the zonal direction and their interaction with waves. Here, we show that significant trends are also found for zonal-mean meridional circulations. First, let us look at the trends in zonal-mean meridional winds (Figure 6). In the tropics in ND, significant positive trends are found around the tropical tropopause, and negative trends are located in the middle and lower tropical troposphere, with statistical significance above 95%. In the extratropics, trends are generally positive, except for negative trends near the extratropical surface between 45°N and 65°N. For FM, a band of strong and significant positive trends is around the tropical tropopause and lower stratosphere, with negative trends in the middle and lower tropical troposphere. Statistical significance levels of these trends are above the 95% confidence level. In the extratropics, negative trends are in the

middle and upper troposphere, and the positive trends are near the surface between 40°N and 65°N, opposite to that in ND.

The trends in zonal-mean meridional winds strongly imply significant changes in mean meridional circulations, i.e., the Hadley circulation in the tropics and the Ferrel circulation in the extratropics. Figure 7a and b show trends in zonal (Eulerian) mean mass streamfunction for ND and FM, respectively. To show the changes in the Hadley cell across the equator, the plots are extended to 45°S. In calculating the mass streamfunction, negative sign is defined for clockwise circulation in the meridional plane. Therefore, in Figure 7a and b the negative trends over the equator and in the northern tropics indicate the intensified northern branch of the Hadley circulation, and the positive trends in the southern tropics mean the intensified southern branch. In ND, the intensification is mainly in the middle and upper tropical troposphere, while the lower part of the Hadley cell show some weakening. In FM, the overall Hadley cell is intensified, and the intensification is much stronger in FM than in ND. The maximum net increase in FM of the mass streamfunction is greater than $40 \times 10^9\ kgs^{-1}$ for the 25 years. It is about 29% of the maximum value of the climatological streamfunction in FM (about $140 \times 10^9\ kgs^{-1}$). It is likely that the intensification of the Hadley cell in both ND and FM is related to observed tropical SST warming.

In the extratropics, trends are negative in ND and positive in FM. Since the Ferrel cell corresponds to positive streamfunctions, these extratropical trends indicate that the Ferrel cell is weakened in ND and strengthened in FM, consistent with the trends in zonal-mean meridional winds in the extratropics shown in Figure 6. It is well known that the Ferrel cell is a thermally indirect, wave-driven mean meridional circulation, and the strength of the streamfunction is determined by the spatial distribution of wave fluxes (See Chapter 10.2 of Holton (1992)). Thus, the opposite trends in the Ferrel cell between ND and FM should be related to the trends in wave activity shown in Figure 5. Though the Eulerian-mean streamfunction is not directly related to EP fluxes, the relation of trends between the Ferrel cell and wave fluxes can be qualitatively explained in terms of the EP flux trends in Figure 5 because the vertical and horizontal EP flux components are equivalent to eddy-heat and eddy momentum fluxes, respectively. Briefly speaking,

since the climatological equatorward EP fluxes and EP flux converegnce in the subtropical troposphere decrease in ND, the corresponding Ferrel cell becomes weakened. In contrast, in FM the climatological equatorward EP fluxes and EP flux convergence are enhanced. It thus leads to the intensification of the Ferrel cell.

2.5. Trends near the surface

Opposite trends between ND and FM are also found near the surface. Figure 8a and b show the 25-year SAT trends for ND, and FM, respectively, derived from the SAT analysis at NASA's Goddard Institute for Space Studies (Hansen *et al.*, 2001). In ND, the SAT trends exhibit cooling over the high-latitude Europe-Asia continent, with maximum cooling of about $-4°$C for the 25 years over Siberia. Warming trends in ND are over the Arctic polar region, particularly Greenland and northern Canada. As shown in many earlier studies, in contrast, in FM SATs display warming trends over the high-latitude Europe-Asia continent and cooling trends over north-eastern Canada. The spatial pattern of SAT trends over high latitudes show striking contrast between ND and FM. The early-winter cooling trends, though statistically less significant, have magnitudes comparable to that of the warming trends in FM.

Figure 9a and b shows the 25-year trends in sea level pressure (SLP) for ND and FM, respectively. For ND, positive trends are located in the polar region, with maximum over northern Europe and Russia. Negative trends are over the extratropics. There are two negative maxima, one over North Atlantic and the other one over North Pacific. For FM, negative trends are over the polar region, with maximum biased toward northern Europe and Russia, and positive trends are over the extratropics, particulalr over oceans. The SLP trends clearly show opposite spatial patterns between ND and FM. It was shown in earlier studies (e.g., Thompson *et al.*, 2000) that the SLP trends in FM are associated with a positive AO trend. This implies that the SLP trends in ND is related to a negative AO trend (the AO index in ND exhibits a weak negative trend over 1978-2002, indeed). Moreover, the spatial pattern of the SLP trends in ND suggests a tendency toward the Eurasian blocking. Thompson and Wallace (2001) pointed out that when the AO is in the low-index phase, it is more likely to form blocking systems, and that blocking systems

slow down the usual eastward propagation of weather systems and lead to intrusion of cold polar air over high-latitude continents and cause cooling. They showed that during 1958-1997 blocking days in the low-index AO phases over Russia are about three times of that in the high-index AO phases (82 days vs. 29 days). This suggests that the continental cooling in ND is related to the increase of Eurasian blocking days (events) upstream. The tendency toward blocking in ND leads to a locally enhancement of southward motion over the Europe-Asia continent. The enhanced southward motion is consistent to the weakening of the lower branch of the Ferrel cell in Figure 6a.

The trends near the surface is dynamically linked to the trends aloft. Wallace and Thompson (2002) have commented that the continental warming in late winter and springtime is related to the acceleration of extratropical zonal winds. From Figiure 3b, one can find that the zonal-wind acceleration extends from the stratosphere to the surface. Wallace and Thompson (2002) also pointed out that when the AO is in the low-index phase, zonal winds are weaker or zonal flows are meandering, and that broader meanders aloft are likely to form blocking systems. From Figure 3a, we have seen the zonal-wind deceleration extending from the stratosphere to the troposphere. It is expected that the SLP tendency toward blocking in ND has close relation to the zonal-wind deceleration aloft.

The blocking signature is usually characterized using 500 mb geopotential heights (D'Andrea *et al.*, 1998). To further demonstrate the tendency toward blocking in ND, and to compare the trends in geopotential heights between ND and FM, we plot the trends in geopotential heights at three levels: 500, 100, and 50 mb. Figure 10a shows the trends in geopotential heights in ND at 500 mb. Positive trends in the polar region and negative trends in the extratropics. The maximum positive trends are over northern Europe, indicating the tendency toward blocking. Comparison of Figure 10a with Figure 9a shows westward and poleward tilting with height of the positive trends. At 100 and 50 mb, positive trends are also in the polar region, wit maximum trends shifting over the opposite side of the Arctic. For FM, the trends at 500 mb have negative maxima over northern Europe and positive maxima over North Atlantic and western Europe, opposite to that in ND. With increasing height, the negative maxima shift eastward from northern Europe to north-eastern Russia. In addition, the trends at 100 and 50 mb show a dipole structure.

3. Discussion and conclusions

We have compared the decadal trends in various fields between ND and FM. In the tropics, the Hadley circulation exhibits strong and significant intensification in both ND and FM, with stronger intenisification in FM. In the extratropics and polar region, trends and their spatial structures are nearly opposite between the early and late winter months. In ND, the trends are characterized by decelerated mean zonal winds, weakened Ferrel cell, enhanced upward wave fluxes associated with reduced equatorward wave fluxes, warming in the polar region in both the troposphere and stratosphere, and SAT cooling over the high-latitude Europe-Asia continent related to the tendency toward Eurasia blocking. In FM, the trends show accelerated zonal winds, strengthened Ferrel cell, reduced upward wave fluxes accompanied by enhanced equatorward wave fluxes, cooling in the polar troposphere and stratosphere, and SAT warming over the high-latitude Europe-Asia continent. The trends in FM are associated with an AO trend toward the high-index polarity, as suggested by earlier studies. While the trends in ND appear to resemble a tendency toward the low-index AO polarity. The magnitudes of trends in ND are slightly weaker than that in FM. The statistical signficance levels for these trends in both ND and FM are close to or above the 95% confidence level in some regions.

These opposite trends in the extratropics raise an important question: What cause the opposite trends between early and late winter months? Comparison of the observed trends with existing GCM simulaion results may be helpful for understanding these questions. The relationship between the trends in the tropics and that in the extratropics illustrated by the spatial pattern of the early-winter trends is rather similar to the simulations by Hou (1998) for testing how the Hadley circulation modulates extratropical climate. Hou (1998) demonstrated that as the tropics is warmed, the Hadley cell is intensified. The stronger Hadley cell transports more angular momentum to the subtropics, thus accelerating the subtropical jet. The stronger jet then leads to increased wave activity and EP flux convergence in the extratropics, which decelerates zonal winds there. Meanwhile, the increase of wave activity enhances eddy-heat transport from midlatitudes to the polar region and causes midlatitude tropospheric cooling and polar warming. The similarity between the observations and simulations suggests a possible impact of the tropics on the extratropics

due to the intensification of the Hadley circulation. The early-winter trends are also partly similar to the GCM simulation results by Butchart *et al.* (2000) and Robinson *et al.* (2002). Butchart *et al.* (2000) showed that increasing greenhouse gases lead to increased wave activity at mid- and high-latitudes and warming in the polar troposphere and stratosphere during winter months. Robinson *et al.* (2002) showed that as observed time-varying SSTs are forced in a GCM, the tropical troposphere shows warming, and the extratropical troposphere responds with cooling and enhanced planetary wave activity in wintertime. The consistency between the above observations in ND and simulations suggests that the early-winter trends in the extratropics and high latitudes might be responses to observed tropical SST warming. On the other hand, GCM simulations on the effect of snow coverage over Siberia on extratropical circulation changes by Gong *et al.* (2003) may provide an alternative interpretation of the observed extratropical trends in ND. They showed that positive snow anomalies in depth and coverage over Siberia in autumn or early winter can force a negative AO, implying that the extratropical trends in ND might be caused by changes in the extratropics.

However, the above consistency fails for FM when the even stronger intensification of the Hadley circulation is accompanied by a decelerated subtropical tropospheric jet and reduced wave activity in the mid- and high-latitudes in late winter. As mentioned in the introduction section, there have been GCM simulation studies to test whether the FM trends are caused by increasing greenhouse gases, tropical SST warming, or stratospheric Arctic ozone depletion. For ozone depletion, while Volodin and Galin (1999) showed that the anomalous continental warming in the early 1990s could be reproduced by imposing observed ozone trend in their GCM, Graf *el al.* (1998) showed that over a longer time period (1979-1997) surface responses to imposed Arctic ozone depletion are weaker than the observed trends, and that the surface responses occur in April and May, about two months later than observed surface trends. The delay of Arctic cooling was also found by Ramaswamy *et al.* (1996) and Langematz *et al.* (2003). The Arctic cooling rate in these simulations, about -2° K per 20 years, is also much weaker than the observed cooling rate of about $-5°$ or $-6°$ K. Therefore, it remains unclear whether the radiative effect of stratospheric ozone depletion alone is sufficient in generating the observed trends in late

winter and springtime, and whether observed trends in January and early February are due to stratospheric Arctic ozone depletion.

For the radiative effect of increasing greenhouse gases, Shindell *et al.* (1999) showed that increasing greenhouse gases are able to generate a positive AO trend comparable to the observed AO trend. They proposed that increasing greenhouse gases cause warming in the tropical and midlatitude troposphere and cooling in the stratosphere, which enhance the meridional temperature gradient near the midlatitude tropopause. The enhancement of temperature gradients leads to accelerated zonal winds in the extratropics, which tend to refract planetary waves equatorward, and cause a positive AO trend and associated continental warming. However, Gillett *et al.* (2002) found that the AO trend due to increasing greenhouse gases is weaker than observations. Moreover, Butchart *et al.* (2000) showed that increasing greenhouse gases lead to increased wave activity at mid- and high-latitudes and warming in the polar troposphere and stratosphere, which implies a negative AO trend.

Model simulations with tropical SST forcing also yielded conflicting results. While Horeling *et al.* (2001) showed that tropical SST warming leads to a positive NAO trend, with negative geopotential height trends in the polar region and positive geopotential height trends in the extratropics, Fyfe *et al.* (1999) and Schneider *et al.* (2003) found no significant AO or NAO trends in geopotential heights from tropical SST forcing. Moreover, Robinson *et al.* (2002) showed that tropical SST forcing generates a Pacific-North-America pattern in the winter season, with positive trends in geopotential heights in the polar region and negative trends in the extratropics, which are nearly opposite to the results by Horeling *et al.* (2001). Butchart *et al.* (2000) and Schneider *et al.* (2003) speculated that these divergent results on the effects of increasing greenhouse gases and tropical SST forcing might be model dependent.

The meridional structure of the observed temperature trends in Figure 2b seems not to be consistent with the proposed mechanism that the extratropical and high-latitude trends in FM are related to tropical warming due to either increasing greenhouse gases or tropical SST warming. First, Figure 2b shows weak cooling trends in the middle and upper tropical troposphere, rather than warming. Second, the mid-latitude warming in the

upper troposphere, contrasted with the cooling in the nearly same region in ND, is related to enhanced eddy-heat fluxes from the subtropics to midlatitudes and is not necessarily a result of greenhouse warming. The disagreements or nearly opposite results of these GCM simulations and the inconsistency between the simulations and observations leave unanswered the question of how increasing greenhouse gases and tropical SST warming can lead to climate changes in the extratropics and high latitudes in FM.

As we know, there are no simulations reporting such a robust contrast of trends between ND and FM. One reason is probably because most of them used the conventional seasonal average, i.e., averaging over December-January-February. Such a seasonal averaging would obviously obscure the contrast of trends between early- and late-winter months. Therefore, it is important for future simulations to separately test the possible forcing for trends in early- and late-winter months. Considering that the effects of increasing greenhouse gases or tropical SST warming persist all winter, it is even more important to identify how these effects can possibly lead to the observed opposite trends in early- and late-winter months, and how late-winter trends are dynamically linked to trends in early-winter months.

Acknowledgments Y. Hu is supported by NASA's Atmospheric Chemistry Modeling and Analysis Program and by NSF. K.K. Tung's research is supported by NSF under grants ATM01-32737 and ATM9813770. NCEP/NCAR Reanalysis data is provided by the NOAA-CIRES Climate Diagnostics Center, Boulder, Colorado, USA, from the Web site at http://www.cdc.noaa.gov/.

References

Andrews, D. G., J. R. Holton, and C.B. Leovy, C. B., 1987: *Middle Atmosphere Dynamics*, Academic Press, New York, NY, 1987, pp.489.

Baldwin, M. P., and T. J. Dunkerton, 2001: Stratospheric Harbingers of Anomalous Weather Regimes. *Science* **294**, 581–584.

Butchart, N., J. Austin, K.R., Knight, A.A. Scaife, and K.L. Gallani, 2000: The Response of the stratospheric climate to projected changes in the concentrations of well-mixed greenhouse gases from 1992 to 2051. *J. Climate*, **13**, 2142–2159.

Coughlin, K., and K. Tung, 2004: Tropospheric wave response to descending decelerations in the stratosphere. Submitted to *J. Geophys. Res.*

D'Andrea, F. and Co-authors, 1998: Northern Hemisphere atmospheric blocking as simulated by 15 atmospheric general circulation models in the period 1979-1988. *Climate Dynamics*, **14**, 385–407.

Fyfe, J. C., G.J. Boer, and G.M. Flato, 1999: The Arctic and Antarctic oscillations and their projected changes under global warming. *Geophys. Res. Lett.*, **26**, 1601–1604.

Graf, H.-K., I. Kirchner, and J. Perlwitz, 1998: Changing lower stratospheric circulation: The role of ozone and greenhouse gases. *J. Geophys. Res.*, **103**, 11251–11261.

Gillett, N. P., and Coauthors, 2002: How linear is the Arctic oscillation response to greenhouse gases. *J. Geophys. Res.*, **107**, 10.1029/2001JD000589.

Gong, G., D. Entekhabi, and J, Cohen, 2003: Modeled Northern Hemisphere winter climate response to realistic Siberian snow anomalies. *J. Climate*, **16**, 3917–3931.

Hansen, J. E., and Co-authors, 2001: A closer look at United States and global surface temperature change. *J. Geophys. Res.*, **106**, 23947–23963.

Hartmann, D. L., J.M. Wallace, V. Limpasuvan, V., D.J.W. Thompson, and J.R. Holton, 2000: Can ozone depletion and greenhouse warming interact to produce rapid climate change. *Proc. Nat. Acad. Sci.*, **97**, 1412–1417.

Hoerling, M. P., W. Hurrell, and T. Xu, 2001: Tropical origins for recent North Atlantic climate change. *Science*, **292**, 90–92.

Holton, J., 1992: *An introduction to Dynamic Meteorology.* 3rd Ed., Academic Press, New York, p.511.

Hu, Y., and K. Tung, 2002: Interannual and decadal variations of planetary-wave activity, stratospheric cooling, and Northern-Hemisphere annular mode. *J. Climate* **15**, 1659–1673.

Hu, Y., and K. Tung, 2003: Possible ozone induced long-term changes in planetary wave activity in late winter. *J. Climate* **16**, 3027-3038.

Hurrell, M. 1995: Decadal trends in the North Atlantic Oscillation region temperatures and precipitation. *Science*, **269**, 676–679.

Kodera, K., and H. Kuroda, 2000: Tropospheric and stratospheric aspects of the Arctic Oscillation. *Geophys. Res. Lett.*, **27**, 3349–3352.

Kushner, P. K., and L. M. Polvani, 2003: Stratosphere-troposphere coupling in a relatively simple AGCM: The role of Eddies. To appear in *J. Climate.*

Jones, P. D., M. New, D.E. Parker, S. Martin, and I.G. Rigor, 1999: Surface air temperature and its changes over the past 150 years. *Rev. Geophs.*, **37**, 173–199.

Labitzke, K., and B. Naujokat, 2000: The lower Arctic stratosphere in winter since 1952. *SPARC Newsl.*, **15**, 11–14.

Langematz, U., and Co-authors, 2003: Thermal and dynamical changes of the stratosphere since 1979 and their link to ozone and CO_2 changes. *J. Geophs. Res.,*, **108**, 10.1029/2002JD0002069.

Newman, P. A., Gleason, J. F., McPeters, R. D., and R.S. Stolarski, 1997: Anomalously low ozone over the Arctic. *Geophys. Res. Lett.*, **24**, 2689–2692.

Pawson, S., and B. Naujokat, 1999: The cold winter of the middle 1990s in the northern lower stratosphere. *J. Geophys. Res.*, **104**, 14209–14222.

Ramaswamy, V., Schwarzkopf, M. d., and W.J., Randel, 1996: Fingerprint of ozone depletion in the spatial and temporal pattern of recent lower-stratospheric cooling. *Nature*, **382**, 616–618.

Randel, W. J. and F. Wu, 1999: Cooling of the Arctic and Antarctic polar stratospheres due to ozone depletion. *J. Climate*, **12,** 1467–1479.

Randel, W. J., F. Wu, and R. Stolarski, 2002: Changes in column ozone correlated with the stratospheric EP flux. *J. Meteorol. Soc. Japan*, **80**, 849-862.

Schneider, E.K., Bengtsson, L., and Z. Hu, 2003: Forcing of Northern Hemisphere climate trends. *J. Atmos. Sci.*, **60**, 1504–1521.

Shindell, D. T., R.L. Miller, G.A. Schmidt, and L. Pandolfo, 1999: Simulation of recent northern winter climate trends by greenhouse-gas forcing. *Nature*, **399**, 452–454.

Thompson, D. W. J., Wallace, J. M., and G.C. Hegerl, 2000: Annular modes in the extratropical circulation, Part II: Trends. *J. Climate*, **13**, 1018–1036.

Thompson, D. W. J., and Wallace, J. M., Regional climate impacts of the Northern Hemisphere annular mode. *Science*, **293**, 85–89, 2001.

Volodin, E. M., and V. Ya. Galin, 1999: Interpretation of winter warming on Northern-Hemisphere continents in 1977-94. *J. Climate*, **12**, 2947–2955.

Wallace, J. M., and D.W.J. Thompson, 2002: Annular modes and climate prediction. *Physics Today*, **55**, 29–33.

Waugh, D. W., Randel, W. J., Pawson. S., Newman, P. A. & Nash, E. R. Persistence of the lower stratospheric polar vortices. *J. Geophys. Res.,* **104,** 27191-27202 (1999).

Zhou, S., A. Miller, J. Wang, J., and J.K., Angell, 2001: Trends of NAO and AO and their associations with stratospheric processes. *Geophy. Res. Lett.* **28**, 4107–4110.

Corresponding address: Yongyun Hu, Columbia University, 2880 Broadway, 112th Street, MC0201, New York, NY 10025. (e-mail: yhu@giss.nasa.gov)

Received _____

Figure captions:

Figure 1: 25-year trends in global zonal-mean temperatures at 50 mb. Color shading interval is 1.0 K per 25 years. In all the figures of this paper, dashed contours indicate student t-test values for trends, and contour 2 approximately corresponds to the 95% confidence level.

Figure 2: Trends in zonal-mean temperatures. (a) ND, (b) FM. Color shading interval is 1.0 K per 25 years.

Figure 3: Trends in zonal-mean zonal winds. (a) ND, (b) FM. Color shading interval is 1.0 ms^{-1} per 25 years.

Figure 4: Trends in squared refractive indices for wavenumber 1. (a) ND, (b) FM. The index square is multiplied by the square of Earth's radius, a^2. Color interval is 10 m^2 per 25 years. To avoid extremely large values of the refractive indices in the subtropics and near the pole where the linear wave theory is no longer valid, the plot is limited between 30°N and 70°N.

Figure 5: Trends in EP fluxes. (a) ND, (b) FM. The white arrows denote trends in EP flux vectors, and the color shading indicates trends in EP flux divergence. Both EP flux vectors and EP divergence are divided by the background air density to make them visible at high levels. The scaling length of the arrows, 1 inch, represents 1.0×10^8 $m^3 s^{-2}$ per 25 years. To illustrate the changes in EP fluxes in the vertical direction, the vertical component of EP fluxes is multiplied by 100. Color interval of the trends in EP flux divergence is 20 $m^2 s^{-2}$ per 25-year. Dashed contours indicate student t-test values for the trends in E-P flux divergence.

Figure 6: Trends in zonal-mean meridional winds. (a) ND, (b) FM. Color shading interval is 0.1 ms^{-1} per 25 years.

Figure 6: Trends in mean meridional mass streamfunction. (a) ND, (b) FM. Color shading interval is 5×1.0^9 kgs^{-1} per 25 years.

Figure 8: Trends in SATs. (a) ND, (b) FM. Color interval is 1.0 K per 25 years.

Figure 9: Trends in sea level pressure. (a) ND, (b) FM. Color shading intervals is 1.0

mb per 25 years.

Figure 10: Trends in geopotential heights. The left panels are for ND. The right panels are for FM. From top to bottom, the plots show trends in geopotential heights at 500, 100, and 50 mb. Units for the color shading intervals are meters per 25 years.

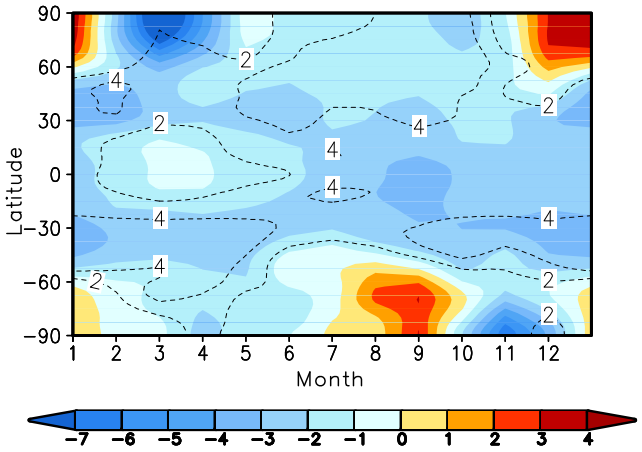

Figure 1.

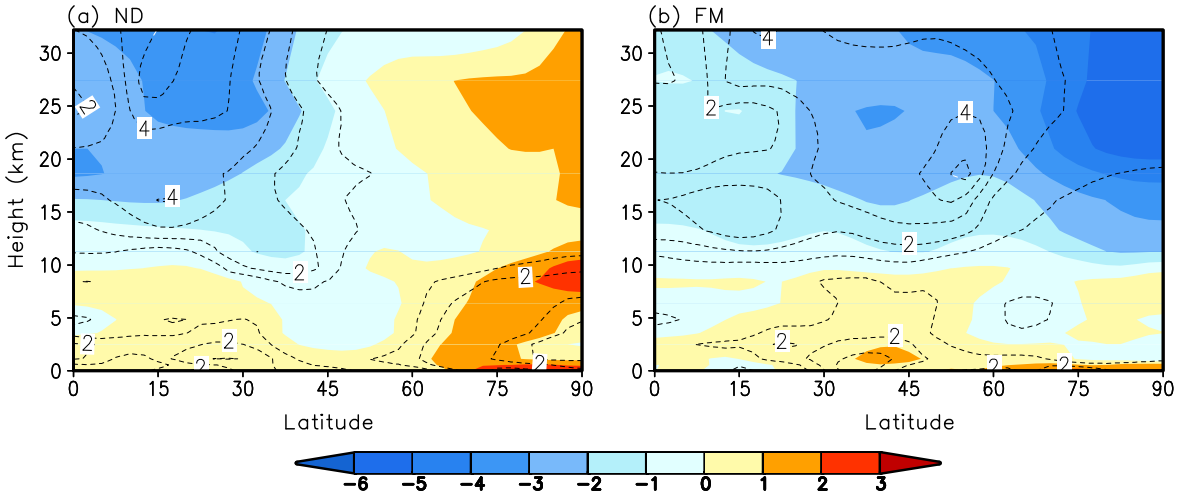

Figure 2.

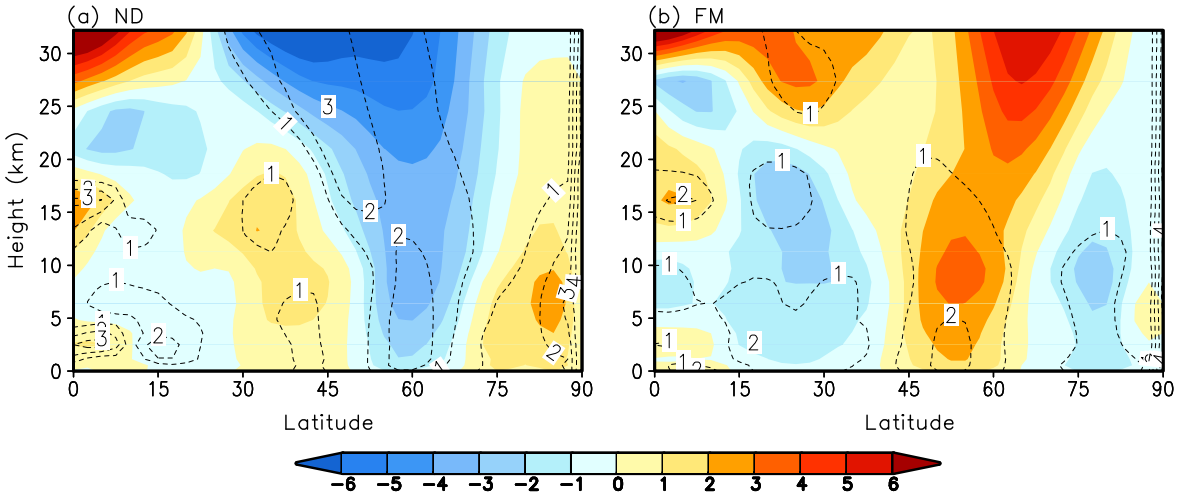
(a) ND
(b) FM
Height (km)
Latitude
Latitude
0
5
10
15
20
25
30
0
15
30
45
60
75
90
−6 −5 −4 −3 −2 −1 0 1 2 3 4 5 6

Figure 3.

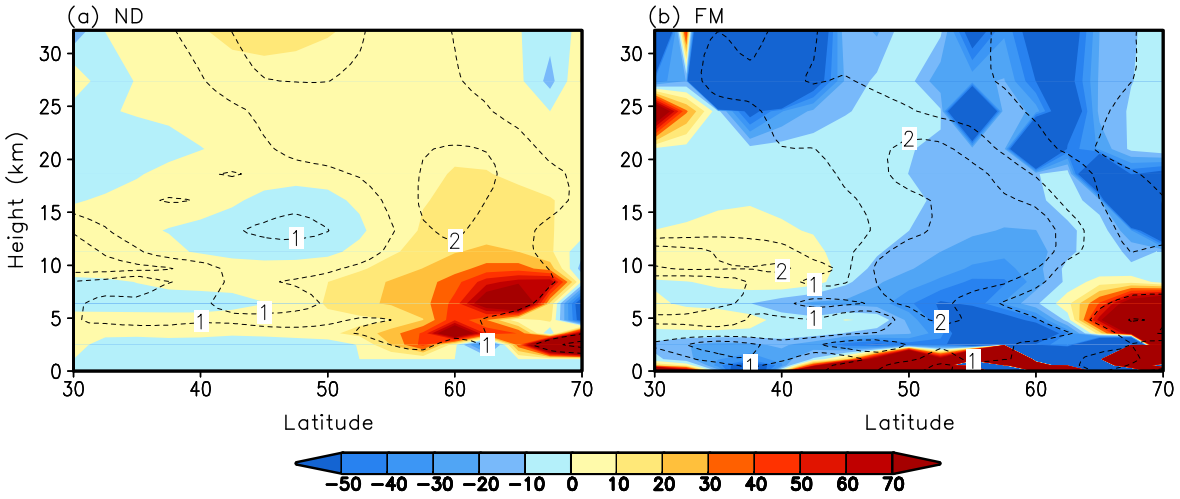

Figure 4.

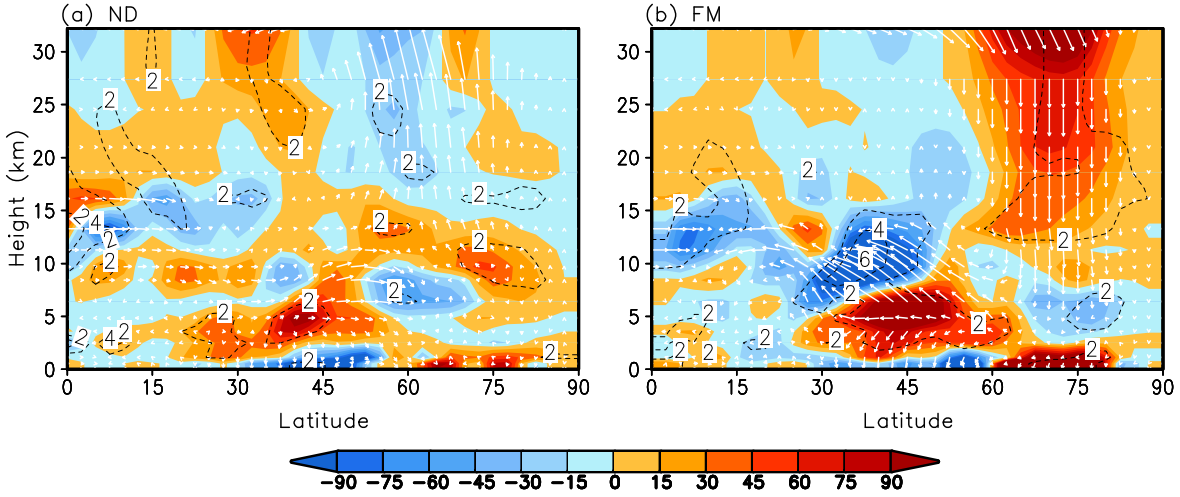

Figure 5.

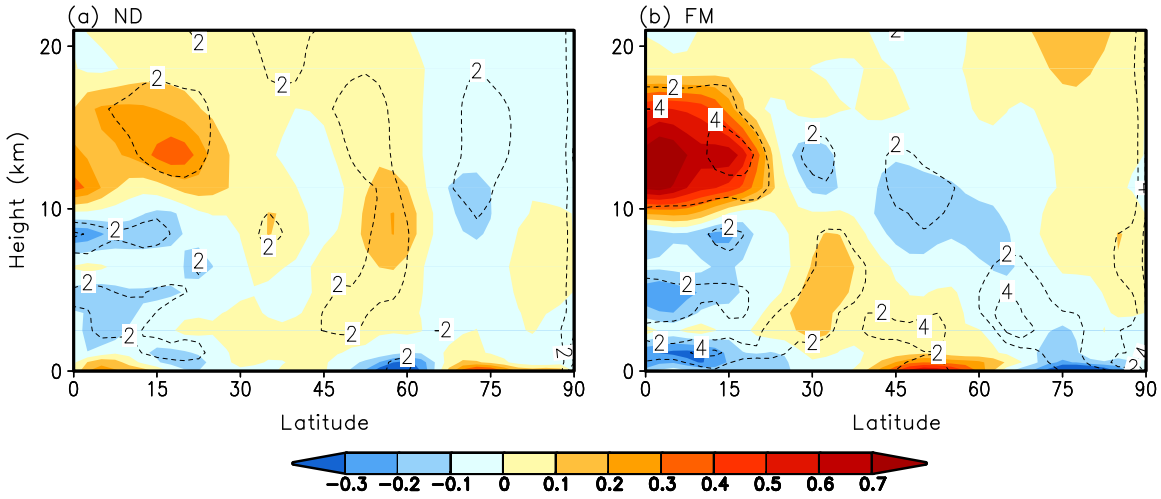

Figure 6.

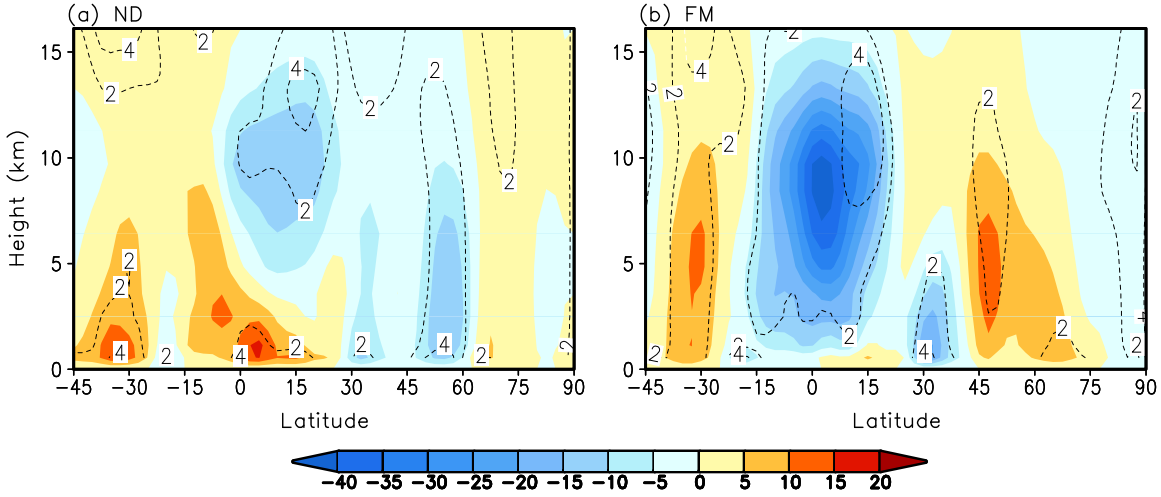

Figure 7.

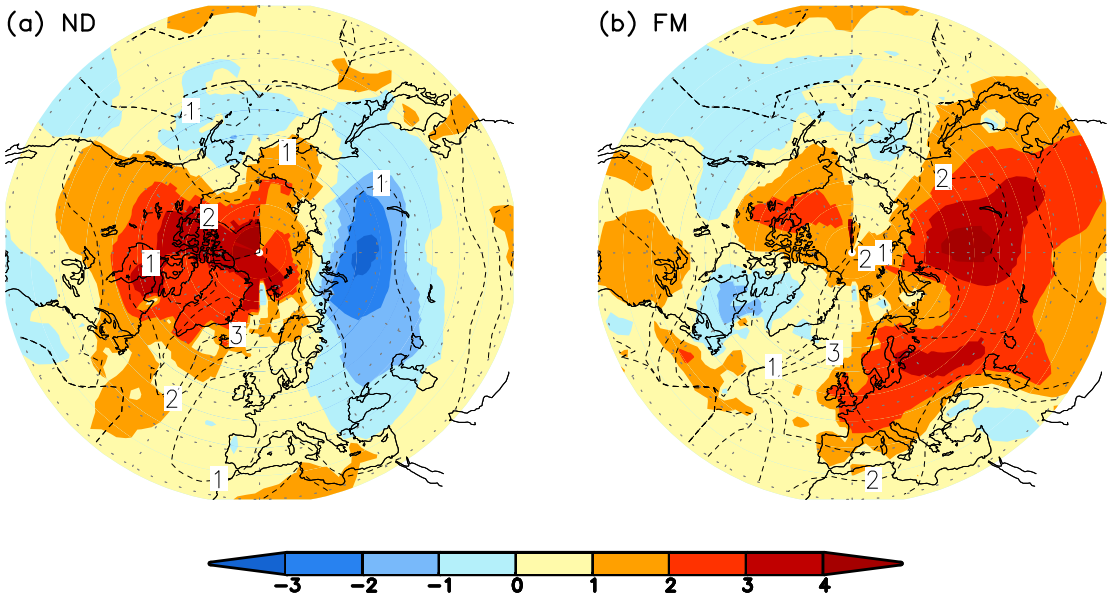

Figure 8.

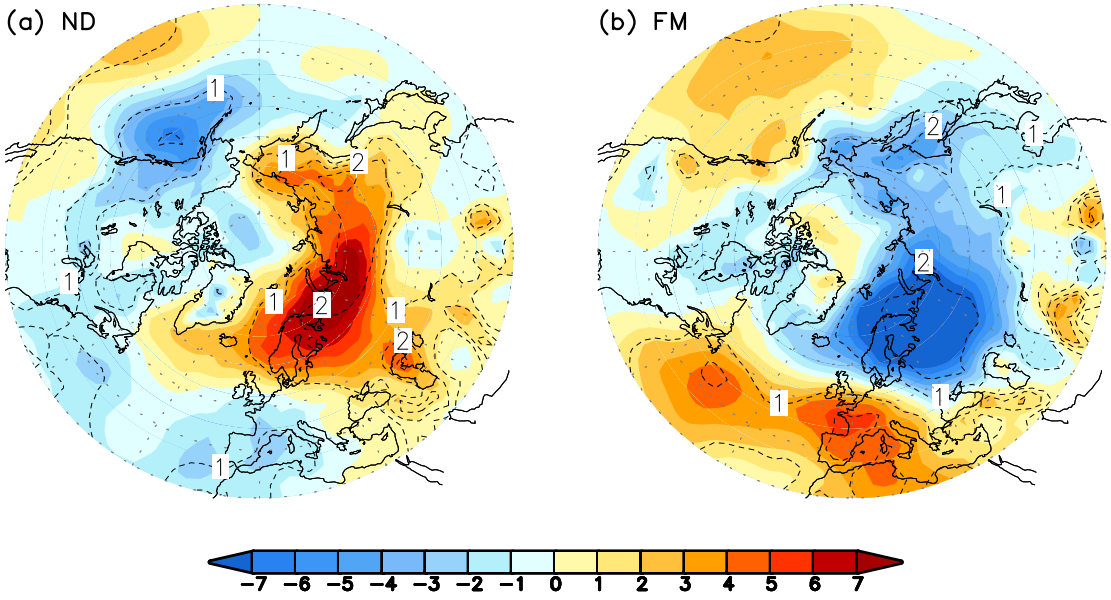

Figure 9.

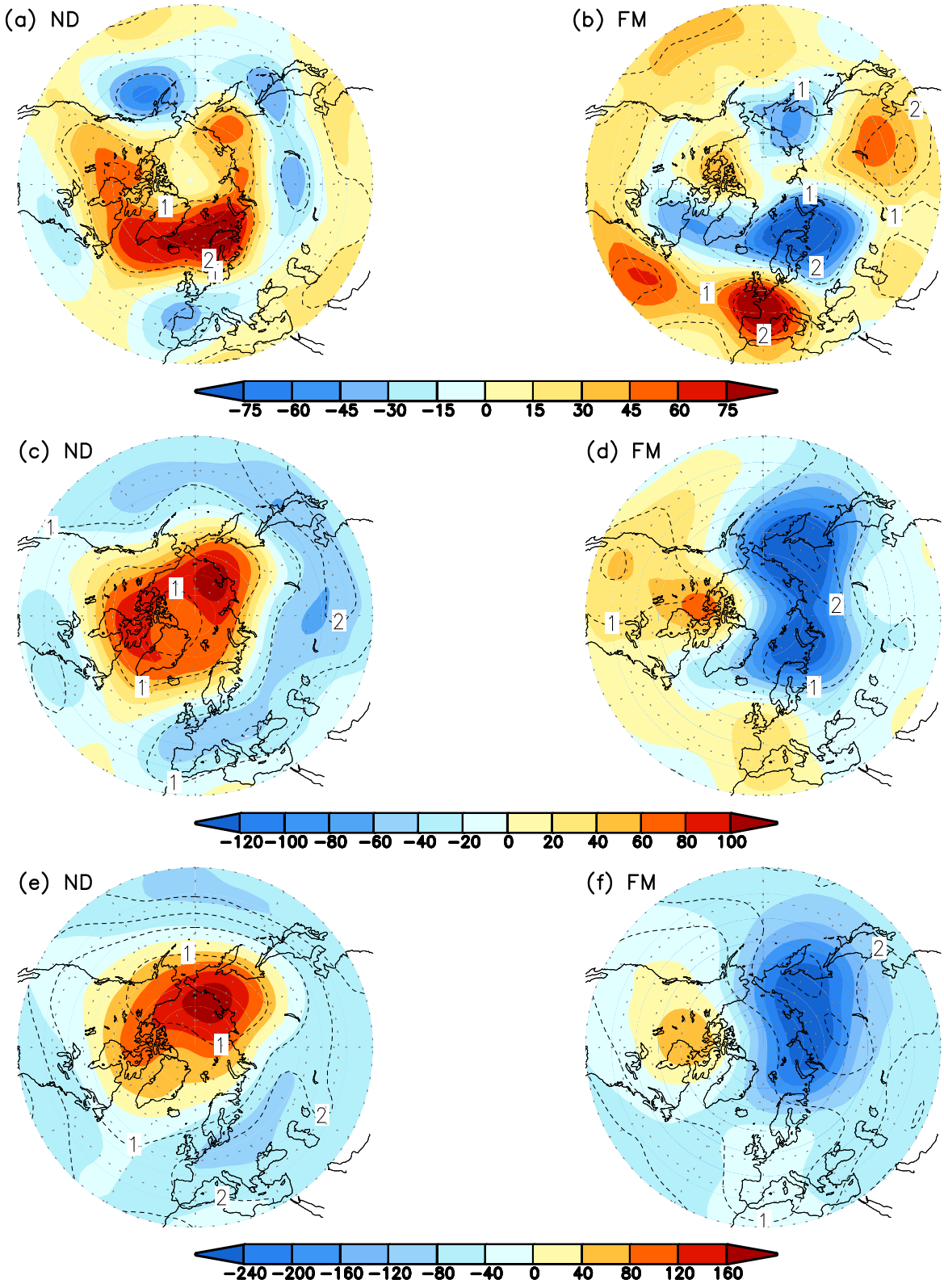
(a) ND
(b) FM
−75 −60 −45 −30 −15 0 15 30 45 60 75
(c) ND
(d) FM
−120 −100 −80 −60 −40 −20 0 20 40 60 80 100
(e) ND
(f) FM
−240 −200 −160 −120 −80 −40 0 40 80 120 160

Figure 10.